Blue Light Generation of Strongly Focused Gaussian Beams by Frequency Doubling of Nd:GSAG Laser

X. Wang, Frank Kallmeyer, S. Wang, Hans J. Eichler, Adalbert M. G. Ding, and Zhiguo Zhang

***Abstract*—Frequency doubling of a focused Gaussian beam involves phase mismatching due to beam divergence. The conversion efficiency was calculated by integration second-harmonic (SH) field along the energy flow propagation path. The resulting SH field spatial distribution was discussed. We demonstrated the generation of blue light in critically type-I phase-matched LiB_3O_5 by frequency doubling of a diode-pumped electrooptic Q-switched Nd:GSAG laser at room temperature. Pulsed blue light with 8-mJ energy and 300-ns pulse duration at 471 nm was generated with 19-mJ incident radiation at 10 Hz. The maximum conversion efficiency was 42%. The experimental results agree well with our calculations.**

***Index Terms*—Focusing Gaussian beam, high energy, second-harmonic generation (SHG).**

I. Introduction

THERE has been great interest in blue laser emission for applications such as underwater communications, high-density data optical storage, and medical diagnostics. Laser diode (LD) pumped, frequency-doubled Nd^{3+} lasers at 470–480 nm are useful for these applications.

Fan and Byer [1] first introduced the diode-pumped quasi-three-level 946-nm Nd:YAG laser at room temperature in 1987, which provided an important way to realize blue light generation by second-harmonic generation (SHG) [2]. A continuous-wave (CW) output power of 4.6 W at 457 nm has been achieved for an intracavity frequency-doubled Nd:YVO_4 laser [3]. Although CW lasers are useful for applications such as display technology or holography, pulsed lasers are needed in special cases such as underwater communication, remote sensing, or material interaction processing. An obvious way of realizing such laser sources is given by frequency doubling a Q-switched Nd:YAG laser that operates at 946 nm [4]. In our laboratory, a passively Q-switched microchip Nd, Cr:YAG laser at 946 nm was built; combined with an external frequency doubler to obtain 473 nm pulses [5].

Manuscript received August 20, 2008; revised November 05, 2008. Current version published May 28, 2009.

X. Wang, F. Kallmeyer, S. Wang, H. J. Eichler, and A. Ding are with the Institut für Optik und Atomare Physik, Technische Universität Berlin, Berlin 10623, Germany (e-mail: wangxinnnn@hotmail.com; frank.kallmeyer@tu-berlin.de; anskina@hotmail.com; eichler@physik.tu-berlin.de; ding@physik.tu).

Z. G. Zhang is with Beijing National Laboratory for Condensed Matter Physics, Institute of Physics, Chinese Academy of Sciences, Beijing 100080, China (e-mail: zgzhang@aphy.iphy.ac.cn).

Color versions of one or more of the figures in this paper are available online at http://www.ieeexplore.ieee.org.

Digital Object Identifier 10.1109/JQE.2009.2013207

A flash lamp-pumped laser, Q-switched with an acousto-optic modulator, produced 40 mJ pulses at 946 nm, but only 2.5 mJ pulses at 473 nm were achieved [6]. The maximum blue energy of 9 mJ at 473 nm was obtained by external doubling frequency an active Q-switched Nd:YAG laser pumped by a Cr:LiSAF laser [7]. As we know, the quasi-three-level nature of the 946-nm transition results in a very small stimulated emission cross section and significant temperature-dependent reabsorption loss from the laser ground state [8]. These features make it difficult to realize high-energy pulse operation.

In this paper, we report an efficient frequency-doubling system for blue light generation. High-energy fundamental wave emission was obtained by an active Q-switched, quasi-CW laser diode (LD) end pumped Nd:GSAG laser. A pulse energy of 20 mJ at 942 nm was achieved at a pump power of 300 mJ with 10 Hz repetition rate. By frequency doubling in a 15-mm-long LiB_3O_5, a maximum output of 8.2 mJ [300 ns, full-width at half-maximum (FWHM)] was obtained at 471 nm. The conversion efficiency from the corresponding Q-switched fundamental output to blue output is 42%. The peak power of the Q-switched blue pulse is up to 28 kW.

II. Theory

SH generation by Gaussian laser beams was already discussed in previous theories [9]–[12]. And also some commercial software involving this problem was designed [13]. But in all of them the wave vector of the fundamental wave is considered to be constant within the whole beam volume. In the case of strong focusing, the crystal length is comparable with the Rayleigh length and phase front is far from the plane, so the local wave vectors of the noncentral beam region are not along the beam axis anymore and the value of the beam vector will not be constant, that means the phase mismatching must be considered. Some authors, for example Kleinman and others[14], [15] and Dreger and McIver [16], also considered this influence, but they only give some overall methods to consider this phase mismatch. In our theory, a numerical method is used, which allows us to calculate the phase mismatch point by point within the nonlinear crystal.

A. Basic Idea

As shown in Fig. 1, a slow, slow–fast type-I SHG process [17] takes place in a biaxial LiB_3O_5 (LBO) crystal. The length of the nonlinear crystal is L, and its cross section is much larger than the input laser beam. We ignore any reflections at the crystal surfaces and also the absorptions of the material. The spatial profile of the input beam is Gaussian and the beam axis is normal to the crystal surface. The coordinates x–y–z are crystallographic

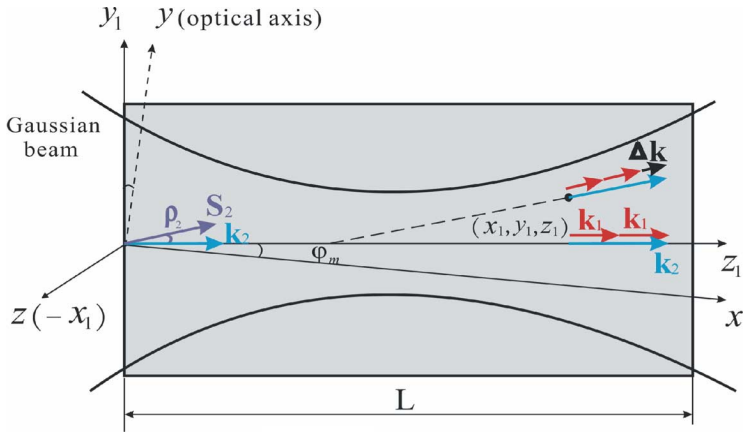

Fig. 1. Propagation of a focused Gaussian beam inside a nonlinear crystal. The local wave vectors of fundamental beam k_1 and SH beam k_2 are perpendicular to the respective phase fronts. In the center of the incident beam the phase matching condition $2k_1 = k_2$ is fulfilled. $\Delta\ k$ is the noncenter wave vector mismatch. The crystal axes x and y lie in the y_1–z_1 plane.

coordinates and x_1–y_1–z_1 are Gaussian beam propagation coordinates. The input surface of the crystal is at $z_1 = 0$. For type-I SHG, φ_m is the phase-matching angle and ρ_2 is the spatial walkoff angle between the input fundamental beam and the output second-harmonic (SH) beam. For perfect phase matching the polarization of the input field is taken along z, and the SH field is polarized in the x–y plane. $\mathbf{k}_1$ is the wave vector at point (x_1, y_1, z_1), and it is perpendicular to the phase front.

The fundamental field is assumed as Gaussian both spatially and temporally. The basic idea is that the fundamental and SH beam are regarded as uncorrelated bundles of curved rays; and the SH field outside the crystal is treated as the integral of the contributions from all the source points inside the crystal. Therefore, the fields at point (x_1, y_1, z_1) inside the nonlinear crystal are written as

$$\mathbf{E}_1(x_1, y_1, z_1, t) = \frac{1}{2}(\mathbf{A_1}(x_1, y_1, z_1, t)e^{-i\mathbf{k}_1\bullet\mathbf{z}_1} + c.c.) \tag{1a}$$

$$\mathbf{E}_2(x_1, y_1, z_1, t) = \frac{1}{2}(\mathbf{A_2}(x_1, y_1, z_1, t)e^{-i\mathbf{k}_2\bullet\mathbf{z}_1} + c.c.) \tag{1b}$$

$$\mathbf{A}_1(x_1, y_1, z_1, t) = \frac{\mathbf{A_{10}}}{1 - i\tau(z_1)} \cdot \exp\left(\frac{(-x_1^2 + y_1^2)}{w_0^2(1 - i\tau(z_1))}\right)\exp\left(\frac{-t^2}{\tau_p^2}\right) \tag{1c}$$

$$\tau(z_1) = \frac{2(z_1 - z_0)}{b} \tag{1d}$$

$$b = w_0^2\frac{2\pi n_1}{\lambda_1}. \tag{1e}$$

Here, $\mathbf{E}$ is the total field, $\mathbf{A}$ is the complex amplitude; $\mathbf{k}_1(x_1, y_1, z_1), \mathbf{k}_2(x_1, y_1, z_1)$ are local wave vectors of the fundamental and SH wave. Specifically, $\mathbf{k}_1$ is orthogonal to the wavefronts of the incident Gaussian beam; $\mathbf{k}_2$ is the wave vector of the SH wave which is generated at point (x_1, y_1, z_1) and has the same direction as $\mathbf{k}_1$ but a slightly different value due to a different refractive index. w_0 and z_0 are the fundamental beam waist and its position inside nonlinear crystal, respectively; τ_p is the Gaussian pulse width. According to the SHG theory, the polarization field excited by the fundamental field is

$$\begin{aligned}\mathbf{P}_{\mathrm{NL}}(x_1, y_1, z_1) &= 2\varepsilon_0\mathbf{d}\cdot\mathbf{E}_1(x_1, y_1, z_1, t)\mathbf{E}_1(x_1, y_1, z_1, t)\\ &= \frac{\varepsilon_0}{2}\mathbf{d}\cdot\mathbf{A}_1^2(x_1, y_1, z_1, t)\cdot e^{-i2\mathbf{k}_1\bullet\mathbf{z}_1} + c.c.\\ &= \frac{1}{2}(\mathbf{P}_2(x_1, y_1, z_1, t)\cdot e^{-i2\mathbf{k}_1\bullet\mathbf{z}_1} + c.c.).\end{aligned} \tag{2}$$

Here, ε_0 is the permittivity of free space and d is the second-order polarization tensor. The amplitude of the polarization field is

$$\mathbf{P}_2(x_1, y_1, z_1, t) = \varepsilon_0\mathbf{d}\cdot\mathbf{A}_1^2(x_1, y_1, z_1, t). \tag{3}$$

The fundamental beam divergence angle is in the range of tens of mrad. So only the main component of the electric field amplitude is considered, which is much larger than the other two components. For type-I SHG in LBO the resulting polarization component is

$$\begin{aligned}P_{2z_1}(x_1, y_1, z_1, t) &= \varepsilon_0 d_{\mathrm{eff}} A_{1x_1}^2(x_1, y_1, z_1, t)\\ &= \varepsilon_0 d_{\mathrm{eff}}\cdot\frac{A_{10x_1}^2}{[1 - i\tau(z_1)]^2}\\ &\quad\cdot\exp\frac{-2(x_1^2 + y_1^2)}{w_0^2(1 - i\tau(z_1))})\exp\left(\frac{-2t^2}{\tau_p^2}\right)\end{aligned} \tag{4}$$

where d_{eff} is the effective nonlinear coefficient. This polarization field generates an SH field

$$\begin{aligned}d\mathbf{A}_2(x_1, y_1, z_1, t) &= dA_{2y_1}(x_1, y_1, z_1, t)\cdot\mathbf{e}_{y_1}\\ &= -i\frac{\omega_1\mu_0 c}{n_{2\omega}}\cdot P_{2z_1}(x_1, y_1, z_1, t)\\ &\quad\cdot\exp(-i\Delta k_{z_1}\cdot z_1)\cdot dz_1\cdot\mathbf{e}_{y_1}\\ &= -i\kappa\frac{A_{10x_1}^2}{[1 - i\tau(z_1)]^2}\exp\left(\frac{-2(x_1^2 + y_1^2)}{w_0^2(1 - i\tau(z_1))}\right)\\ &\quad\cdot\exp\left(\frac{-2t^2}{\tau_p^2}\right)\exp(-i\Delta k_{z_1}\cdot z_1)\cdot dz_1\cdot\mathbf{e}_{y_1}\end{aligned} \tag{5}$$

where ω_1 is the circular frequency of the fundamental wave, μ_0 is the permeability of the free space, c is speed of light in vacuum, and $n_{2\omega}$ is the refractive index for SH polarization. We start from a point at the entrance surface and add all incremental SH amplitudes expressed by (5) along energy propagation pass ($\mathbf{S}_2$-direction as indicated in Fig. 1). If the fundamental beam propagates inside the crystal as a strongly focused Gaussian beam and $\mathbf{E}_1$ is not always along the z-axis, then for LBO type-I SHG not only the SH beam but also the fundamental beam has a double refraction angle between the $\mathbf{k}$ vector and the $\mathbf{S}$ vector. After passing through the whole crystal, the final SH field amplitude at the $z_1 = L$ plane can be described by an integral over the crystal length

$$\begin{aligned}\mathbf{A}_2(x_{1L}, y_{1L}, L, t) &= A_{2y_1}(x_{1L}, y_{1L}, L, t) \cdot \mathbf{e}_{y_1} \\ &= \mathbf{e}_{y_1} \cdot \int_0^L dA_{2y_1}(x_1, y_1, z_1, t). \quad (6)\end{aligned}$$

Then, the SH energy can be obtained by an integral over the x_1–y_1 output plane and over time

$$\begin{aligned}U_{\mathrm{SH}} = \frac{1}{2}\varepsilon_0 c n_{2\omega} \int_{-\infty}^{\infty} dt \int_{-\infty}^{\infty} dx_{1L} \\ \times \int_{-\infty}^{\infty} dy_{1L} |\mathbf{A}_2(x_{1L}, y_{1L}, L, t)|^2. \quad (7)\end{aligned}$$

B. Spatially Dependent Phase Mismatch

Starting from a point in the entrance surface of nonlinear crystal and dividing the crystal length into n integration cells, the phase mismatching factor $\exp(-i\triangle k_{z1}(x_1, y_1, z_1)z_1)$ for the point (x_1, y_1) in plane z_1 is related to the phase-matching angle θ, φ (the angles between $\mathbf{k}_1$ and the z-axis, and the projection of $\mathbf{k}_1$ in the x–z plane and the $x$axis), and $\theta_{\mathrm{m}} = \pi/2, \varphi_{\mathrm{m}}$ are the perfect phase-matching angles. The relationships between these angles are shown in Fig. 2(a) and (b).

Rewrite (5) as follows:

$$\begin{aligned}&d\mathbf{A}_2(x_1, y_1, z_1, t) \\ &= -i\kappa \left\{ \frac{A_{10x_1}^2}{1 - i\tau(z_1)} \exp\left(\frac{-2(x_1^2 + y_1^2)}{w_0^2(1 - i\tau(z_1))} \right) \right. \\ &\quad \left. \cdot \exp\left(\frac{-2t^2}{\tau_p^2} \right) \right\} \cdot \frac{1}{1 - i\tau(z_1)} \\ &\quad \times \exp(-i\Delta k_{z_1} \cdot z_1) \cdot dz_1 \cdot \mathbf{e}_{y_1}. \quad (8)\end{aligned}$$

We noticed that except the phase mismatching part the amplitude enclosed in the brackets $\{\}$ has the Gaussian form. It is concluded that the total field A_2 has approximately a corresponding Gaussian form. The phase mismatch factor is then calculated by

$$\theta(x_1, y_1, z_1) = \theta_m - \alpha'(x, y, z) = \frac{\pi}{2} + \alpha'(x_1, y_1, z_1) \quad (9a)$$

$$\alpha'(x_1, y_1, z_1) = \frac{x_1}{R_{zr}(x_1, y_1, z_1)} \quad (9b)$$

$$\varphi(x_1, y_1, z_1) = \varphi_m + \beta'(x_1, y_1, z_1) \quad (9c)$$

$$\begin{aligned}\beta'(x_1, y_1, z_1) &= \frac{y_1}{x_1} \cdot tg\alpha'(x_1, y_1, z_1) \quad (x_1 \neq 0) \\ &= \frac{y_1}{R_{zr}(x_1, y_1, z_1)} \quad (x_1 = 0) \quad (9d)\end{aligned}$$

$$\begin{aligned}\Delta k_{z_1}(x_1, y_1, z_1) = &(n_{1\omega}(\theta(x_1, y_1, z_1), \varphi(x_1, y_1, z_1)) \\ &- n_{2\omega}(\theta(x_1, y_1, z_1), \varphi(x_1, y_1, z_1))) \\ &\cdot \cos\alpha'(x_1, y_1, z_1) \\ &\cdot \cos\beta'(x_1, y_1, z_1)) \cdot \frac{4\pi}{\lambda_1}. \quad (9e)\end{aligned}$$

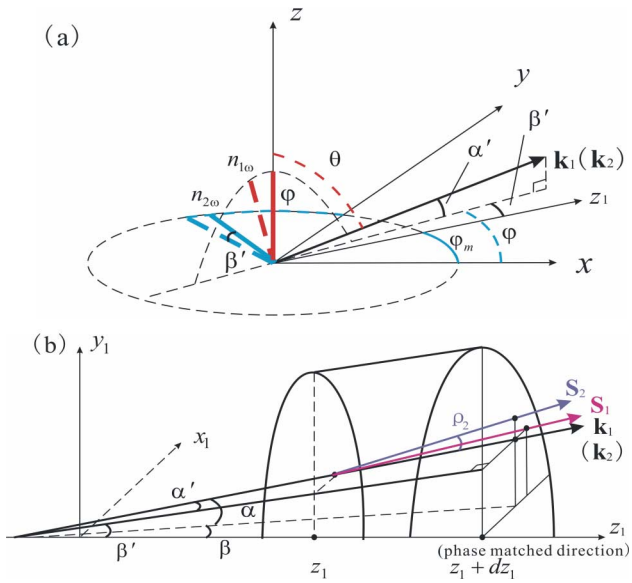

Fig. 2. Relationship between phase matching angle, $\theta_{\mathrm{m}}, \varphi_{\mathrm{m}}$, and propagation angles α, β, β' for the wave vectors $\mathbf{k}_1$ and $\mathbf{k}_2$. (a) Refractive indexes of LBO for arbitrary wave vector direction; (b) spatial propagation within one cell of integration. α: the angle between $\mathbf{k}_1$ and its projection in the x_1–z_1 plane; α': the angle between $\mathbf{k}_1$ and its projection in the y_1–z_1 plane; β: the angle between the projection of $\mathbf{k}_1$ in the x_1–z_1 plane and the z_1-axis; β': the angle between the projection of $\mathbf{k}_1$ in the y_1–z_1 plane and the z_1-axis.

In these expressions, R_{zr} is the radius of the beam wavefront at point (x_1, y_1, z_1). For a Gaussian beam, it can be calculated by

$$\begin{aligned}&R_{zr}(x_1, y_1, z_1) \\ &= \frac{b}{2} \cdot \left(\frac{2z_r(x_1, y_1, z_1)}{b} + \frac{b}{2z_r(x_1, y_1, z_1)} \right) \quad (10a) \\ &z_r(x_1, y_1, z_1) - (z_1 - L/2) \\ &= R_{zr}(x_1, y_1, z_1) \\ &\quad \mp \sqrt{R_{zr}^2(x_1, y_1, z_1) - x_1^2 - y_1^2} \\ &\quad \times \begin{pmatrix} \text{``}-\text{''} : z_1 - L/2 \geq 0 \\ \text{``}+\text{''} : z_1 - L/2 < 0 \end{pmatrix}. \quad (10b)\end{aligned}$$

Knowing the fundamental amplitude $A_{10\times 1}^2$ at this source point, the incremental SH amplitude can be calculated by using (5). For a Gaussian beam the relationship between the fundamental energy U_1 and the amplitude can be given as

$$\begin{aligned}A_{10x_1}^2 &= |\mathbf{A}_{10}|^2 \cdot \cos\alpha'(x_1, y_1, z_1) \cdot \cos\beta'(x_1, y_1, z_1) \\ &\approx |\mathbf{A}_{10}|^2 \\ &= \frac{4U_1}{\pi\tau_p w_0^2 \varepsilon_0 c n_{1\omega}} \quad (11)\end{aligned}$$

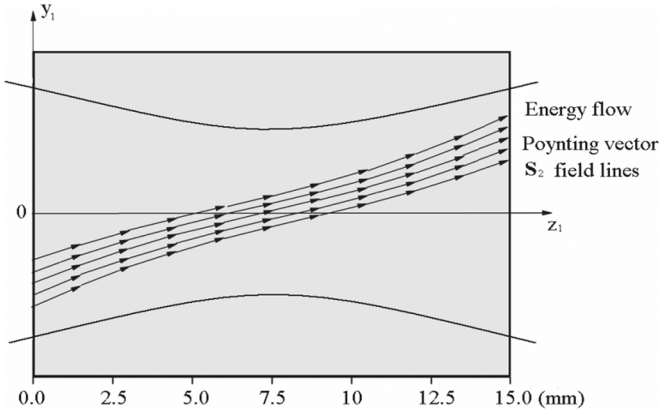

Fig. 3. Sketch of integration paths for the SH field considering beam walkoff.

C. Second Harmonic Energy Flow and Integration Paths

If the beam walkoff angle was involved, for an arbitrary point inside the crystal [as shown in Fig. 2(b)], according to the properties of a biaxial nonlinear crystal, the directions of $\mathbf{k}$ and $\mathbf{S}$ for both the input fundamental beam and the output SH beam are different. We should discuss them individually.The double refraction angle of the fundamental wave is important only in the x_1 direction and will change the spatial distribution of the fundamental beam along z_1. If $x_1 \geq 0$, the displacement is $\triangle x_1 \geq 0$; otherwise, it is $\triangle x_1 < 0$. This means that the distribution of the fundamental wave will become more and more elliptical during propagation and the power density in the x_1-direction will decrease; the overall conversion efficiency also decreases. Double refraction of the SH wave takes place in the y_1- direction and no matter if $y_1 \geq 0$ or $y_1 < 0$ the displacement is $\triangle y_1 \geq 0$, so along its propagation the SH wave will walk away from the fundamental wave. The conversion efficiency will decrease due to the worse overlap.

The influence of the fundamental double refraction is weak because of the small double refraction angle. This means that $\mathbf{S}_1$ is approximately parallel to $\mathbf{k}_1$. So in our calculation only the SH double refraction angle is considered. And because $\mathbf{k}_2$ is nearly parallel to $\mathbf{k}_1$ and $\mathbf{S}_1$, the SH double refraction angle is equal to the spatial walkoff angle between the fundamental beam and the SH beam. In this case, the SH field distribution at $z_1 = L$ should be calculated by integrating (5) along $\mathbf{S}_2$ (ρ_2 line), as shown in Fig. 3.

The coordinate for the neighbored integral cells has the relationship:

$$y_1(z_1 + \Delta z) = y_1(z_1) + \rho_2(x_1, y_1, z_1) \cdot \Delta z \tag{12a}$$

$$x_1(z_1 + \Delta z) = x_1(z_1). \tag{12b}$$

The resulting SH field amplitude at (x_{1L}, y_{1L}, L) can be described as

$$\begin{aligned}\mathbf{A}_2(x_{1L}, y_{1L}, L, t) &= \int_0^L d\mathbf{A}_2(x_1, y_1, z_1, t) \\ &= -i\kappa A_{10x_1}^2 \cdot \exp\left(-\frac{2t^2}{\tau_P^2}\right) \cdot F(x_{1L}, y_{1L}, L) \cdot \mathbf{e}_{y_1}.\end{aligned} \tag{13}$$

The final SH energy can be written as an integral of field intensity over time and the x_1–y_1 plane at $z_1 = L$

$$\begin{aligned}U_{\mathrm{SH}} &= \frac{1}{2}\varepsilon_0 c n_{2\omega} \int_{-\infty}^{\infty} dt \int_{-\infty}^{\infty} dx_{1L} \\ &\quad \times \int_{-\infty}^{\infty} dy_{1L} |\mathbf{A}_2(x_{1L}, y_{1L}, L, t)|^2 \\ &= \varepsilon_0 c n_{2\omega} \frac{\sqrt{\pi}\tau_p \kappa^2 A_{10x_1}^4}{4} \int_{-\infty}^{\infty} dx_{1L} \\ &\quad \times \int_{-\infty}^{\infty} |F(x_{1L}, y_{1L}, L)|^2 dy_{1L}.\end{aligned} \tag{14}$$

The conversion efficiency is

$$\begin{aligned}\eta_{\mathrm{nd}} &= \frac{U_{\mathrm{SH}}}{U_1} \\ &= \frac{4\kappa^2}{\varepsilon_0 c n_{1\omega}} \cdot \frac{U_1}{\pi^{3/2}\tau_p w_0^4} \\ &\quad \cdot \int_{-\infty}^{\infty} dx_{1L} \int_{-\infty}^{\infty} |F(x_{1L}, y_{1L}, L)|^2 dy_{1L}.\end{aligned} \tag{15}$$

It is the efficiency under the nondepleted assumption.

If the beam walkoff and phase mismatching are ignored, we can get a simple analytical solution

$$\eta_{\mathrm{nd}} = \frac{U_{\mathrm{SH}}}{U_1} = \frac{4\kappa^2 n_{2\omega}}{\varepsilon_0 c n_{1\omega}^2} \cdot \frac{U_1 L^2}{\pi^{3/2}\tau_p w_0^2}. \tag{16}$$

This corresponds to (2.99) in Boyd and Kleinman's theory [10]: $\eta = (\boldsymbol{K} P_1 \boldsymbol{L}^2)/(w_0^2)$. P_1 is the fundamental beam power and K is a constant related to the nonlinear coefficient.

D. Including Fundamental Power Depletion

To consider the fundamental power depletion, the simple linear depletion approximation [12] can be used

$$\eta = 1 - \frac{1}{1 + \eta_{\mathrm{nd}}}. \tag{17}$$

It was mentioned in [12] that this approximation ignores the nonlinear reshaping of the fundamental field. In our case, SHG is in the low depletion region, so it can be considered that the strong part of the beam has a similar depletion as the weak part. But for stronger depletion this simple approximation will overestimate the efficiency.

III. Numerical Calculations

The aforementioned model was used to calculate the conversion efficiency at different conditions. The results will be compared with experiment in next section. The constants used in the calculations are for 15 mm LBO that was cut for frequency doubling of 942–471 nm at room temperature. The value of NLO

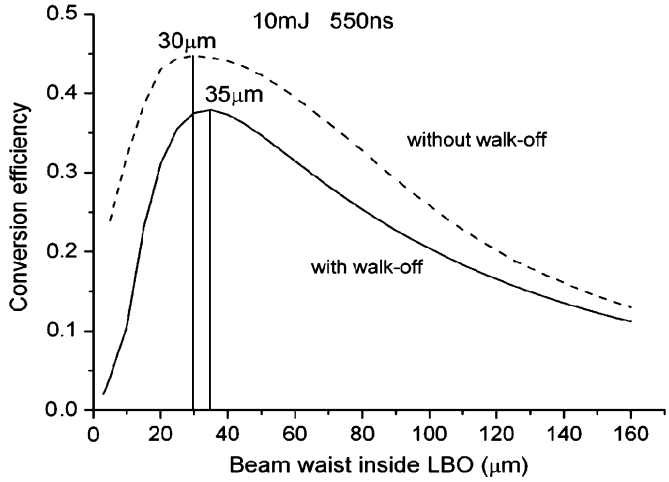

Fig. 4. Calculated conversion efficiency considering and neglecting walkoff angle.

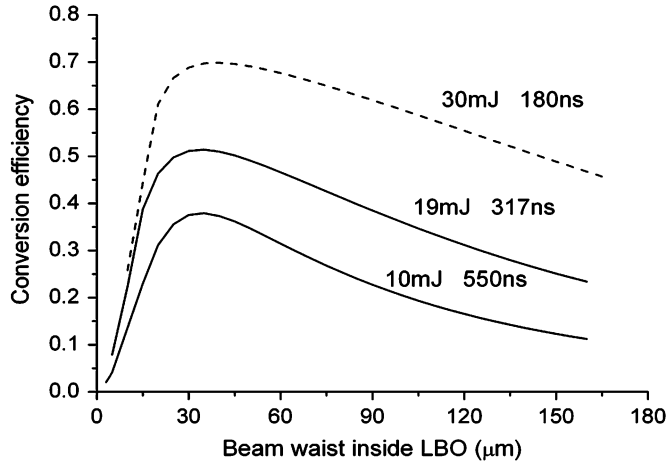

Fig. 5. Calculated conversion efficiency versus beam waist for several input energy and pulse duration used in experiments.

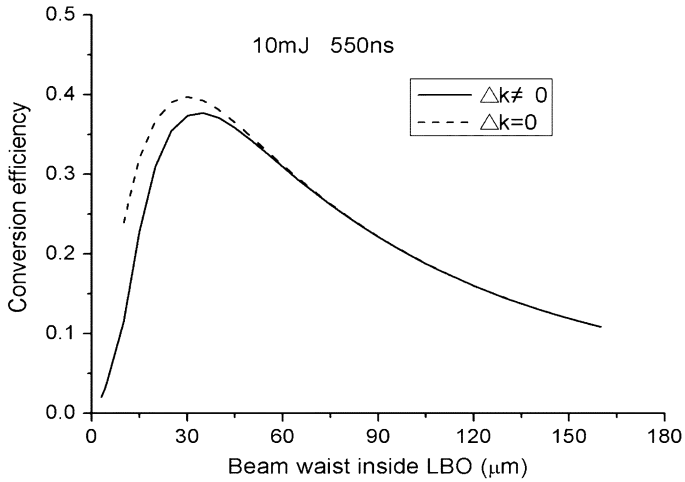

Fig. 6. Calculated conversion efficiency considering and neglecting phase mismatch.

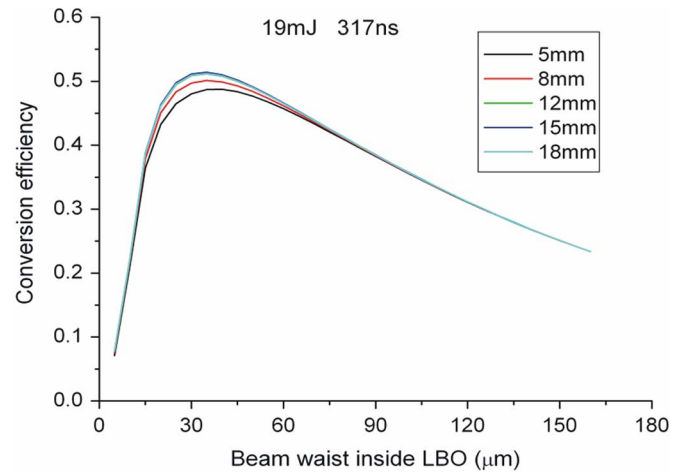

Fig. 7. Optimized crystal length and beam waist calculation.

susceptibility-d_{32} and Sellmeier equations that was used to calculate the refractive index are provided by [18]. The effective nonlinear coefficient type-I phase match in the x–y plane is

$$d_{\text{eff}} = d_{32}\cos\varphi_m = (-0.98 \pm 0.09)\ \text{pm/V} \cdot \cos 19.6^\circ = -0.92 \pm 0.085\ \text{pm/V}.$$

A. Optimum Fundamental Beam Waist Inside the LBO Crystal

The conversion efficiency was calculated as a function of beam waists for 10 mJ fundamental input energy with 550 ns pulse duration (FWHM). The results with and without walkoff are shown in Fig. 4. It shows that in both cases there is an optimized waist (30 μm without walkoff and 35 μm with walkoff) leading to maximum conversion efficiency. The difference of the maximum efficiencies in both cases shows that the influence of the walkoff angle on conversion efficiency should be considered in this case. In Fig. 5, the optimized beam waist was calculated under different input energies. It can be seen that the value of the optimized beam waist keeps constant even though the efficiency increases with the increasing of fundamental energy.

B. Phase Mismatching Due to Beam Divergence

In order to get some knowledge about the influence of nonzero phase mismatching the conversion efficiency was calculated excluding and including $\triangle\mathbf{k}_{z1}$. It can be seen from Fig. 6 that the Gaussian beam phase mismatch has only a slight effect on conversion efficiency especially for bigger input beam waists. But the phase distortion on the far-field SHG spatial distribution can be observed. It will deteriorate the SH beam quality. The details will be shown later.

C. Optimum Crystal Length

The dependence of conversion efficiency versus crystal length was studied. As shown in Fig. 7, the optimized crystal length is 15 mm and the optimized conversion efficiency changes slightly with the crystal length. This means, for a Gaussian beam the part far from the beam waist has only a small contribution to the SH power due to its low power density. Furthermore, it can be seen that the optimized beam waist becomes slightly bigger (40 μm) when the crystal length is quite short (5 mm).

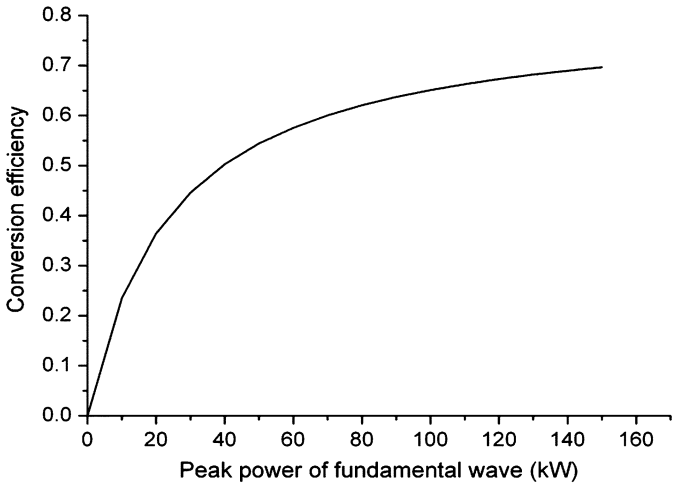

Fig. 8. Power dependence of the optimal SHG efficiency.

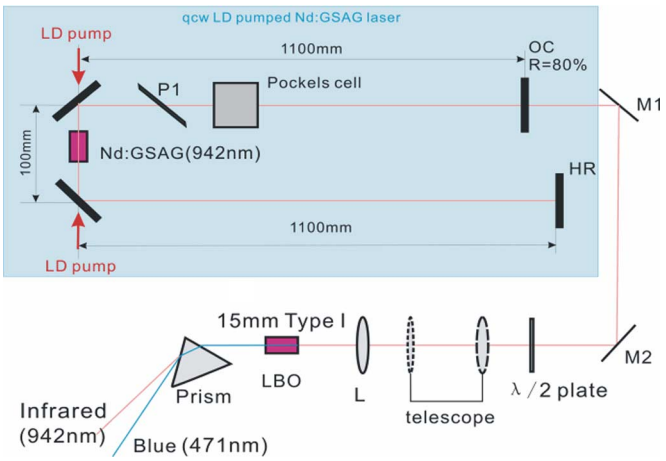

Fig. 9. Setup of the frequency doubling system.

TABLE I
BEAM WAISTS FOR DIFFERENT FOCAL LENGTHS OF FOCUSING LENS L

Focus length (mm)	Beam waist (μm) at 10mJ	Beam waist (μm) at 19mJ
75	24	24
100	31	32
125	39	40
150	47	49
200	63	65
250	79	81
300	95	98
400	128	131
500	160	165

D. Power Dependence of Efficiency

The power dependence of the optimal SHG efficiency is shown in Fig. 8. The optimized beam waist was chosen (35 μm) for efficiency calculation. We noticed that for a high input power the efficiency increases more slowly.

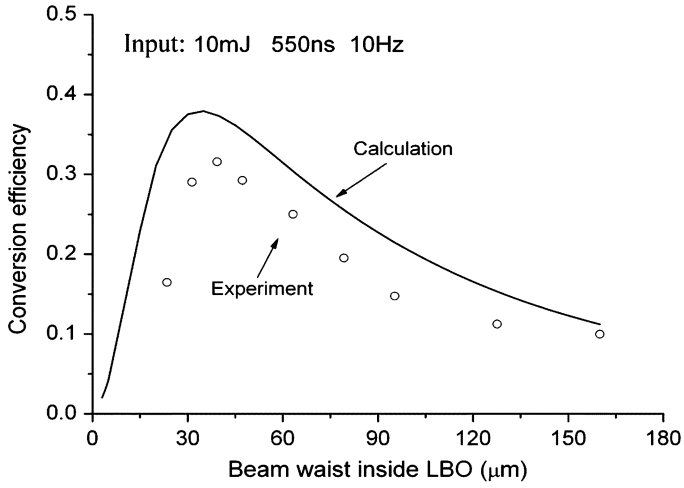

Fig. 10. Experimental conversion efficiency and comparison with numerical calculation.

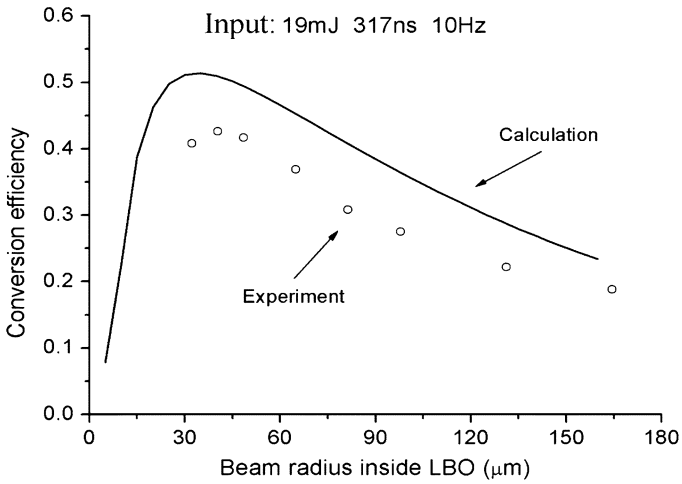

Fig. 11. Experimental conversion efficiency and comparison with numerical calculation.

IV. EXPERIMENTAL RESULTS AND DISCUSSION

In our experiment, the fundamental beam was generated by a double-sided LD-pumped Nd:GSAG laser. The setup is shown in Fig. 9. A Pockels cell was inserted into the cavity to realize an active Q-switch. It was triggered by the pump source, so the repetition rate can be tuned between 1 and 100 Hz. A 2.3-m-long cavity was used to achieve a ~2.00 mm lasing beam diameter inside the active medium to avoid the damage of the laser crystal. The maximum output energy of 28 mJ can be obtained with 10-Hz repetition rate. The beam quality factor is $M^2 < 1.1$.

A 15-mm-long LBO was used as a frequency doubler. The phase-matching angles are $\theta_m = 9°, \varphi_m = 19.6°$, which was cut for 942–471 nm at room temperature. Both surfaces have an antireflective (AR) coating for both wavelengths. The temperature of the LBO was controlled by an active temperature controller. A half-wave plate was used to adjust the input polarization. The SH output was separated from the fundamental input by a prism. A set of simple focus lenses with different focus lengths was used to obtain different beam waists inside

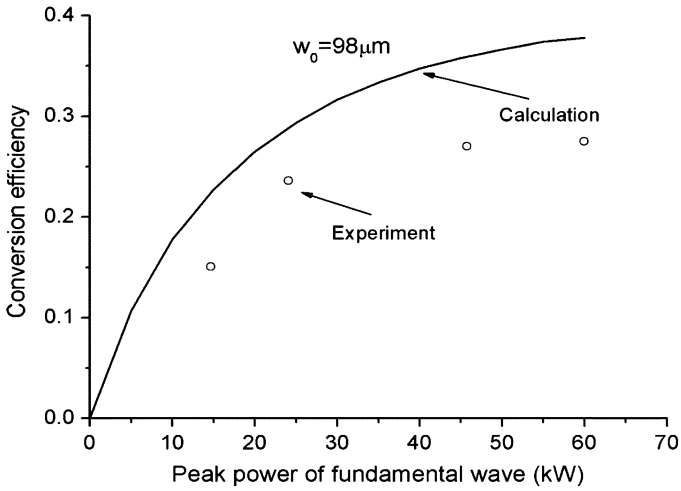

Fig. 12. Conversion efficiency versus input power.

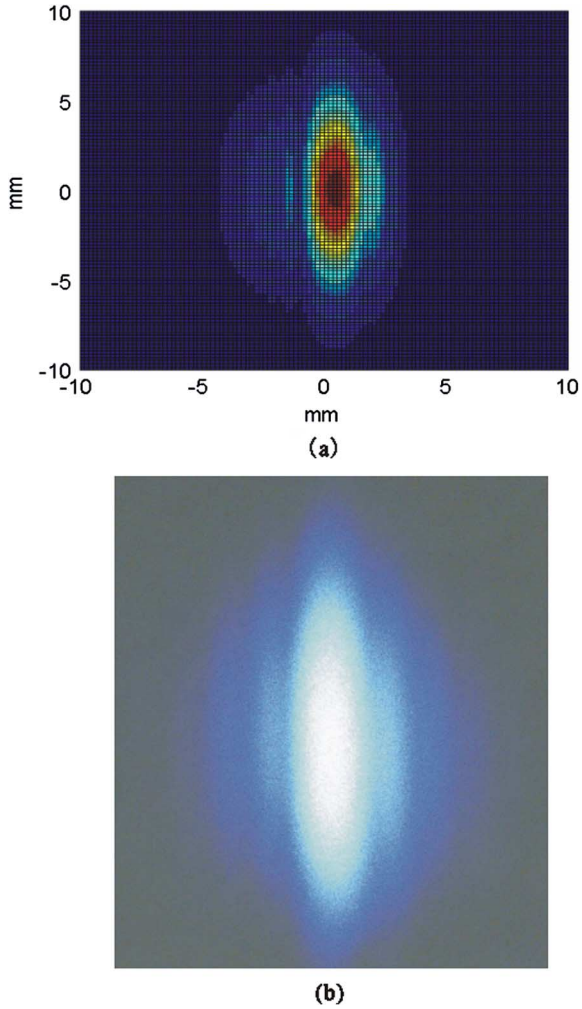

Fig. 13. SHG intensity for a 49-μm input beam waist.

the nonlinear crystal. The corresponding beam waists are listed in Table I.

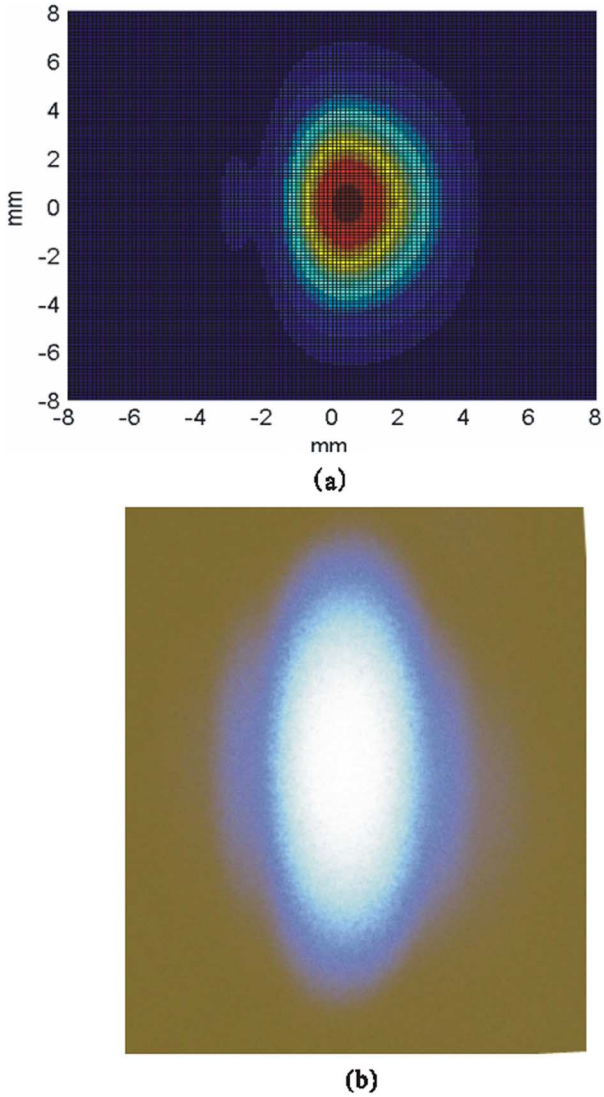

Fig. 14. SHG intensity for a 65-μm input beam waist.

A. *Conversion Efficiency*

First, input pulses with 10 mJ energy, 550 ns pulse duration, and 10 Hz repetition rate were used. A maximum pulse energy of 3.1 mJ blue light was obtained with 31% conversion efficiency. The optimized beam waist was 39 μm, which agrees well with the calculated 35 μm, as already shown in Fig. 4. The experimental results and numerical calculations are shown in Fig. 10.

Then, we increased the fundamental energy to 19 mJ. When a 125-mm focus lens was used, 8-mJ blue light was generated with 317 ns pulse duration (FWHM). The AR coating was destroyed for beam waists smaller than 24 μm. So, in order to increase the energy of the blue beam a crystal without coating or with better coating should be used. The experimental results can be seen in Figs. 11 and 12. In Fig. 12, the overestimation for high input power densities follows from the inaccuracy of the simple depletion approximation. A transmitted fundamental beam with dark central part was observed for high input powers and small beam waists.

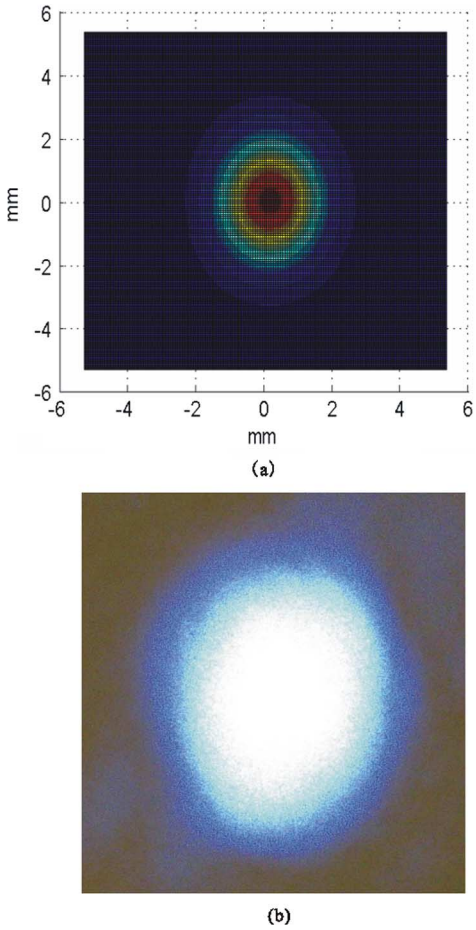

Fig. 15. SHG intensity for a 131-μm input beam waist.

B. Far-Field Second Harmonic Intensity Distribution

It is worth noting that when the beam waist was smaller than 80 μm, the SHG distribution became elliptical—it became smaller in one direction compared with the fundamental distribution and at the same time more and more fringes were observed. The experimental results give our calculations a good prove. The photos and the calculation results are shown in Figs. 13–15 for different beam waists. They show that stronger focusing gives stronger deterioration in the y_1 direction.

V. Conclusion

The efficiency for type-I SH generation in the biaxial nonlinear crystal LBO is analyzed considering the phase mismatching caused by Gaussian propagation inside a nonlinear crystal. In addition, walkoff and pump depletion are considered. The spatial SHG output distribution is calculated for a focused Gaussian input beam. A 15-mm-long LBO was used to realize the generation of blue light by frequency doubling of a diode-pumped electro-optic Q-switched Nd:GSAG laser at room temperature. A pulsed blue beam with 8-mJ energy and 300-ns pulse duration at 471 nm was generated. The incident radiation from the Nd:GSAG laser was 19 mJ at 10 Hz. The maximum conversion efficiency for optimum focusing of the incident beam was 42%. The experimental results agreed well with this theory.

References

[1] T. Y. Fan and R. L. Byer, "Continuous-wave operation of a room-temperature, diode-laser-pumped, 946-nm Nd:YAG laser," *Opt. Lett.*, vol. 12, no. 10, pp. 809–811, Oct. 1987.

[2] J. Hong, B. D. Sinclair, W. Sibbett, and M. H. Dunn, "Frequency-doubled and Q-switched 946-nm Nd:YAG laser pumped by a diode-laser array," *Appl. Opt.*, vol. 31, no. 9, pp. 1318–1321, 1992.

[3] Q. H. Xue, "High-power efficient diode-pumped Nd:YVO_4/LiB_3O_5 457 nm blue laser with 4.6 W of output power," *Opt. Lett.*, vol. 31, no. 8, pp. 1070–1072, 2006.

[4] S. Spiekermann, H. Karlsson, and F. Laurell, "Efficient frequency conversion of a passively Q-switched Nd:YAG laser at 946 nm in periodically poled $KTiOPO_4$," *Appl. Opt.*, vol. 40, no. 12, pp. 1979–1982, 2001.

[5] N. P. Barnes, B. M. Walsh, R. L. Hutcheson, and R. W. Equall, "Pulsed $^4I_{3/2}$ to $^4I_{9/2}$ operation of Nd lasers," *J. Opt. Soc. Amer. B*, vol. 16, no. 12, pp. 2169–2177, 1999.

[6] L. Lv, L. Wang, P. Fu, X. Chen, Z. Zhang, V. Gaebler, D. Li, B. Liu, H. J. Eichler, S. Zhang, A. Liu, and Z. Zhu, "Diode-pumped self-Q-switched single-frequency 946-nm Nd^{3+}, Cr^{4+}:YAG microchip laser," *Opt. Lett.*, vol. 26, no. 2, pp. 72–74, 2001.

[7] W. A. Clarkson, N. S. Felgate, D. C. Hanna, and S. D. Butterworth, "," presented at the Conf. Lasers Electro-Opt., Baltimore, MD, May 23–28, 1999.

[8] W. P. Risk and W. Lenth, "Room-temperature, continuous-wave, 946-nm Nd:YAG laser pumped by laser-diode arrays and intracavity frequency doubling to 473 nm," *Opt. Lett.*, vol. 12, no. 12, pp. 993–995, 1987.

[9] D. A. Kleinman and R. C. Miller, "Dependence of second-harmonic generation on the position of the focus," *Phys. Rev.*, vol. 148, no. 1, pp. 302–312, 1966.

[10] G. D. Boyd and D. A. Kleinman, "Parametric interaction of focused Gaussian light beams," *J. Appl. Phys.*, vol. 39, pp. 3597–3639, 1968.

[11] A. Steinbach, M. Ranner, F. C. Crnz, and J. C. Bergquist, "CW second harmonic generation with elliptical Gaussian beam," *Opt. Commun.*, vol. 123, pp. 207–214, 1996.

[12] H. F. Wang and A. M. Weiner, "Efficiency of short-pulse type-i second-harmonic generation with simultaneous spatial walkoff, temporal walkoff, and pump depletion," *IEEE J. Quantum Electron.*, vol. 39, no. 12, pp. 1600–1618, Dec. 2003.

[13] *SNLO*, [Online]. Available: www.sandia.gov/imr/XWEB1128/xxtal.htm

[14] G. D. Boyd, A. Ashkin, J. M. Dziedzic, and D. A. Kleinman, "Second-harmonic generation of light with double refraction," *Phys. Rev.*, vol. 137, pp. 1305–1309, Dec. 1965.

[15] D. A. Kleinman, A. Ashkin, and G. D. Boyd, "Second-harmonic generation of light by focused laser beams," *Phys. Rev.*, vol. 145, no. 1, pp. 338–379, 1966.

[16] M. A. Dreger and J. K. McIver, "Second-harmonic generation in a nonlinear, anisotropic medium with diffraction and depletion," *J. Opt. Soc. Amer. B*, vol. 7, no. 5, pp. 776–784, 1990.

[17] S. G. Grechin, S. S. Grechin, and V. G. Dmitriev, "Complete classification of interaction types for the second-harmonic generation in biaxial nonlinear crystals," *Quantum Electron.*, vol. 30, no. 5, pp. 377–386, 2000.

[18] D. N. Nikogosyan, "Lithium triborate (LBO). A review of its properties and applications," *Appl. Phys. A.*, vol. 58, no. 3, pp. 181–190, 1994.

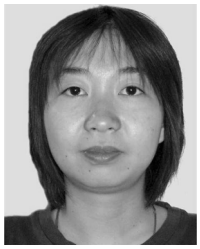

X. Wang was born in Beijing, China, in 1980. She received the B.S. and M.S. degrees in photoelectric engineering from Beijing Institute of Technology, Beijing, China, in 2002 and 2005, respectively. She is currently working toward the Ph.D. degree in Institut für Optik und Atomare Physik, Technische Universität Berlin, Berlin, Germany.

She has authored or coauthored papers on laser diode (LD) pumped solid-state lasers. Her current research interests include LD-pumped high-energy and high-power solid-state lasers and nonlinear optics.

Frank Kallmeyer received the diploma in physics from the Technische Universität Berlin, Berlin, Germany, in 2001.

He is currently a Scientific Coworker with the Institut für Optik und Atomare Physik, Technische Universität Berlin, where he is in charge of the development of diode-pumped solid-state lasers with high power and narrow linewidth.

S. Wang was born in Chengdu, China, in 1982. She received the B.S. degree from the University of Science and Technology of China, Anhui, in 2001. She is currently working toward the Ph.D. degree in solid-state lasers at the Technische Universitaet Berlin, Berlin, Germany.

Hans J. Eichler received the Dipl.-Ing. and the Ph.D. degree from the Technische Universität Berlin, Berlin, Germany, in 1965 and 1967, respectively.

In 1971, he was appointed as a member of the founding board of the University of Paderborn, where he became a Full Professor in 1972. From 1978 to 1980, he was a consultant for industrial laser projects sponsored by the German Minister for Research and Technology. From 1980 to 1983, he spent three sabbatical summers as a Member of the Technical Staff, Bell Laboratories, Holmdel, NJ. He is currently with the Institut für Optik und Atomare Physik, Technische Universität Berlin. His current research interests include gas and solid-state lasers, nonlinear optics, and various laser applications. He has authored or coauthored more than 500 papers published in scientific journals and has coauthored several books.

Prof. Eichler has been the Chairman of the Quantum Optics Association of the German Physics Society, and the Society of Applied Optics since 1982. Since 1985, he has been a member of the Program Committees of the International Laser Conferences held in different cities throughout the United States. He has also contributed to the organization of numerous conferences and summer school courses on applied nonlinear optics.

Adalbert M. G. Ding received the Dipl.-Ing. and the Ph.D. degree from the Technische Universität Berlin, Berlin, Germany, in 1966 and 1968, respectively.

From 1966 to 1971, he was a Scientist with Hahn-Meitner Institute for Nuclear Research, where he was the Head of the Kinematics Group from 1973 to 1989. From 1971 to 1973, he was a Postdoctoral Fellow with the University of Toronto, Toronto, ON, Canada. Since 1989, he has been a Member of the Staff at the Technische Universität Berlin. He was invited as a Guest Professor to several institutes (A.N.U, Canberra, La Trobe University, Melbourne, and the University of New South Wales, Australia; University of Manchester, U.K.; University of Innsbruck, Austria; Beijing Institute of Technology, China). His current research interests include the field of molecular beam experiments, photo-ionization of clusters and large molecules, lasers, and development of optical systems, particularly for the use in solar energy applications. He has authored or coauthored more than 100 publications in refereed journals.

Dr. Ding was a member of numerous advisory committees. He has organized and contributed to numerous international conferences.

Zhiguo Zhang received the Graduate degree from the University of Science and Technology of China, Anhui, in 1964.

From 1964 to 1974, he was a Researcher with the Shanghai Institute of Optics and Fine Mechanics. Since 1974, he has been a Professor with Beijing National Laboratory for Condensed Matter Physics, Institute of Physics, Chinese Academy of Sciences, Beijing. His current research interests include laser physics and nonlinear optics. He has authored or coauthored more than 200 papers published in scientific journals.